Supporting Information

A water-stable La-MOF with high fluorescent sensing and supercapacitive performances

Qian-Qian Liu, Shi-Hui Zhang, Jing Yang, and Ke-Fen Yue*

Key Laboratory of Synthetic and Natural Functional Molecule Chemistry of the Ministry of Education, National Demonstration Center for Experimental Chemistry Education, College of Chemistry and Materials Science, Northwest University, Xi'an 710069, PR China

E-mail address: ykflyy@nwu.edu.cn.

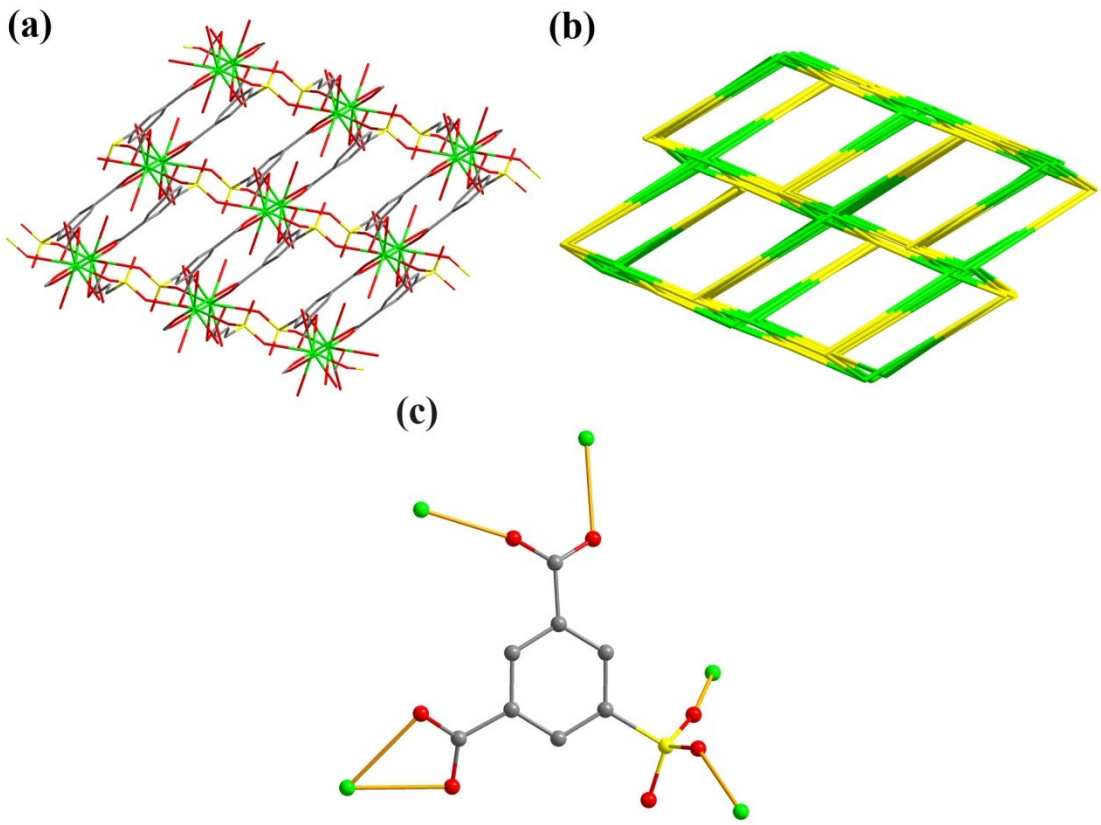

Fig. **S1** (**a**, **b**) Topological net for **La-MOF** and (**c**) Coordination modes of SIP^{3+} ligand.

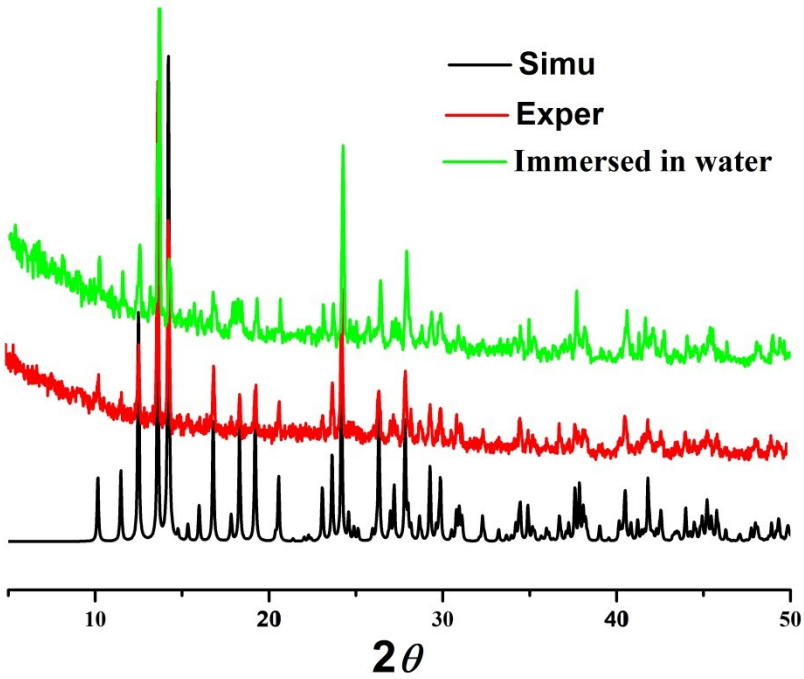

Fig. **S2** PXRD patterns of **La-MOF** immersed in water and as-synthesized products.

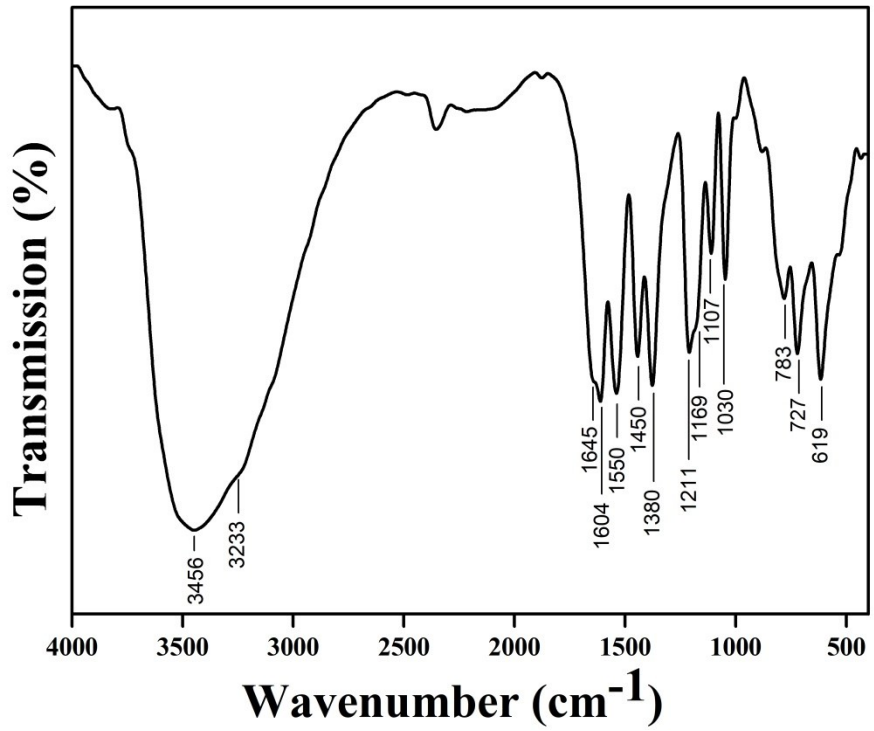

Fig. **S3** The FT-IR spectrum of **La-MOF**.

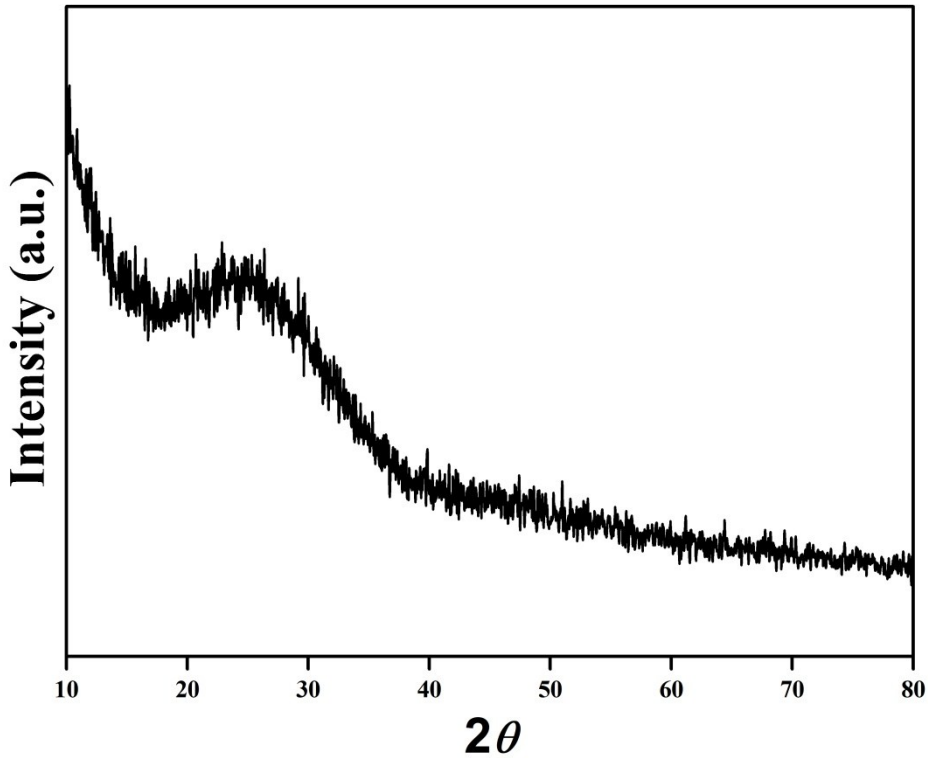

Fig. **S4** PXRD pattern of final product of TG.

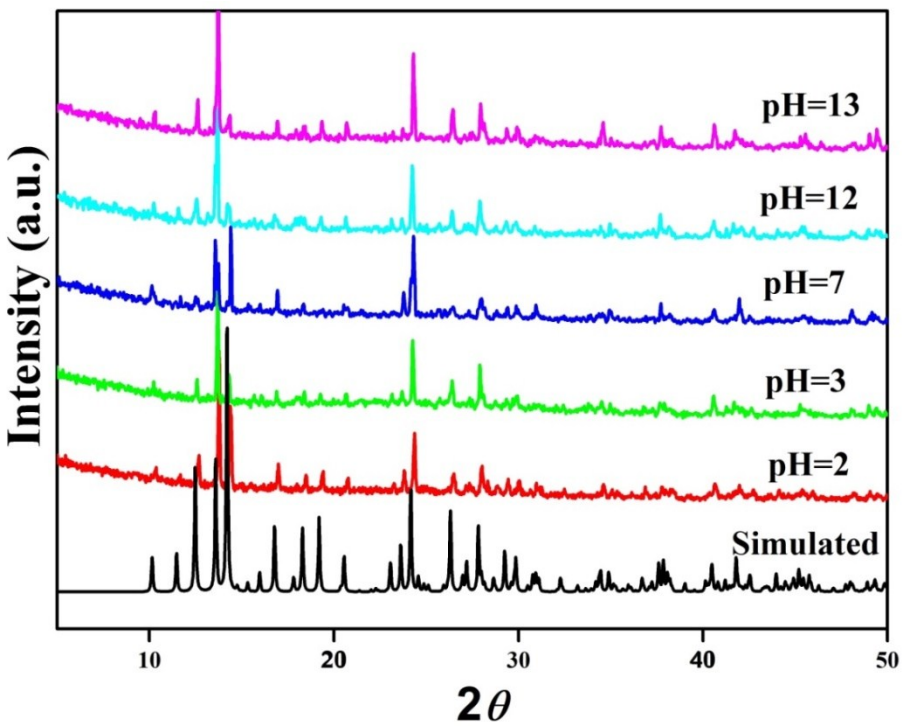

Fig. **S5** PXRD profiles of **La-MOF** after being soaked in water, acidic, and basic solutions.

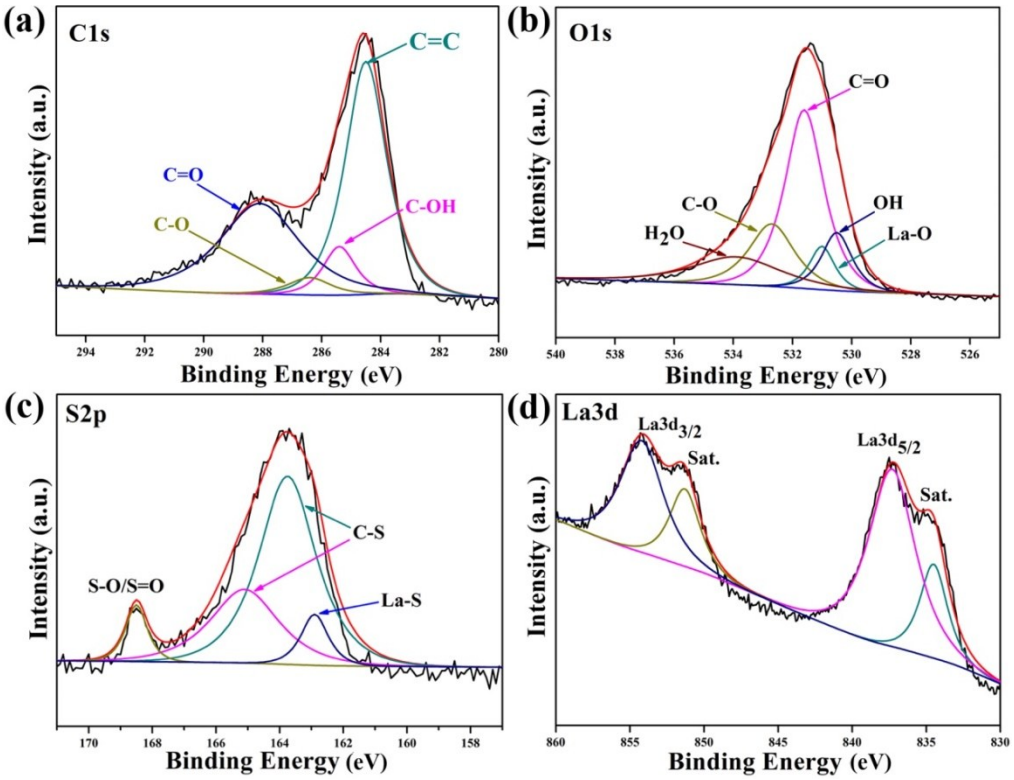

Fig. **S6** XPS high resolution (**a**) C 1s; (**b**) O 1s; (**c**) S 2p; (**d**) La 3d spectra of **La-MOF**.

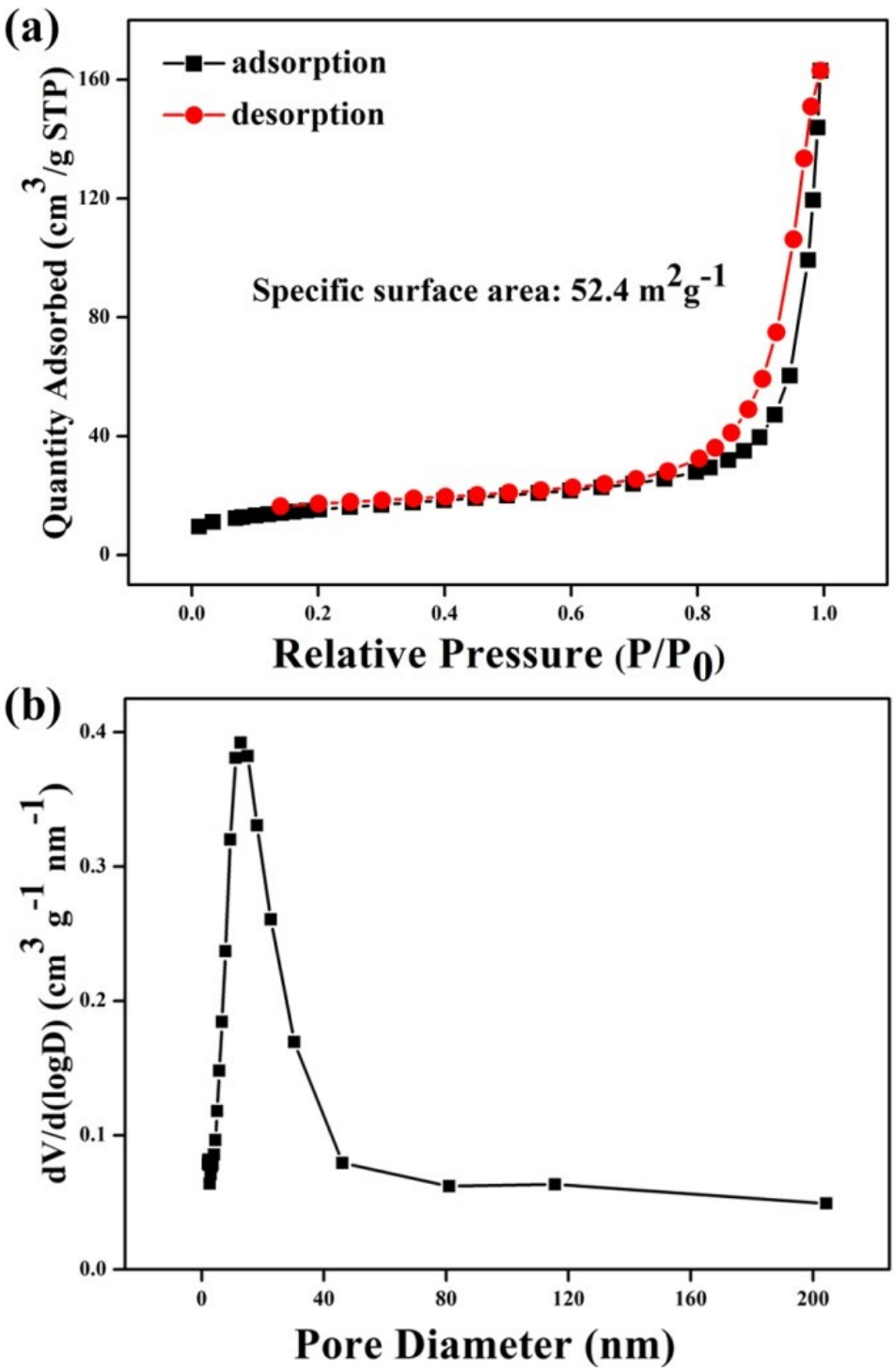

Fig. **S7** View of (**a**) N_2 adsorption-desorption isotherm; (**b**) pore-size distribution curves.

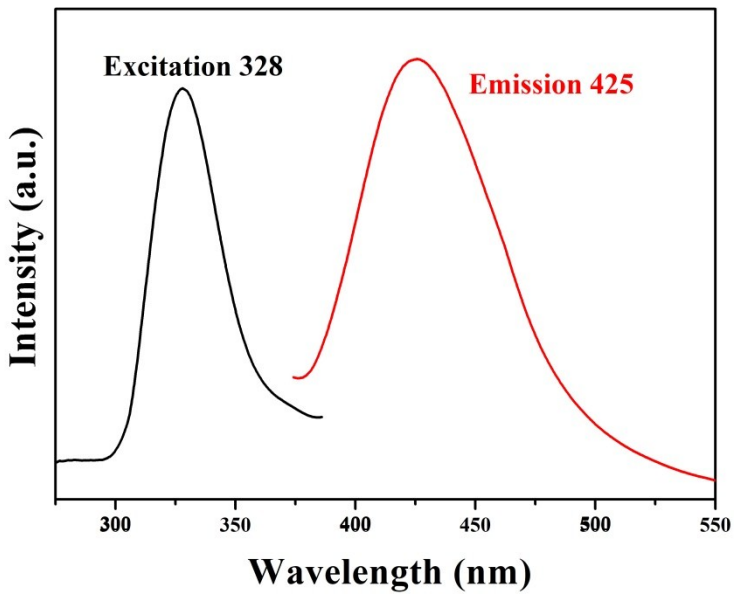

Fig. **S8** The solid-state fluorescence spectra of **La-MOF**.

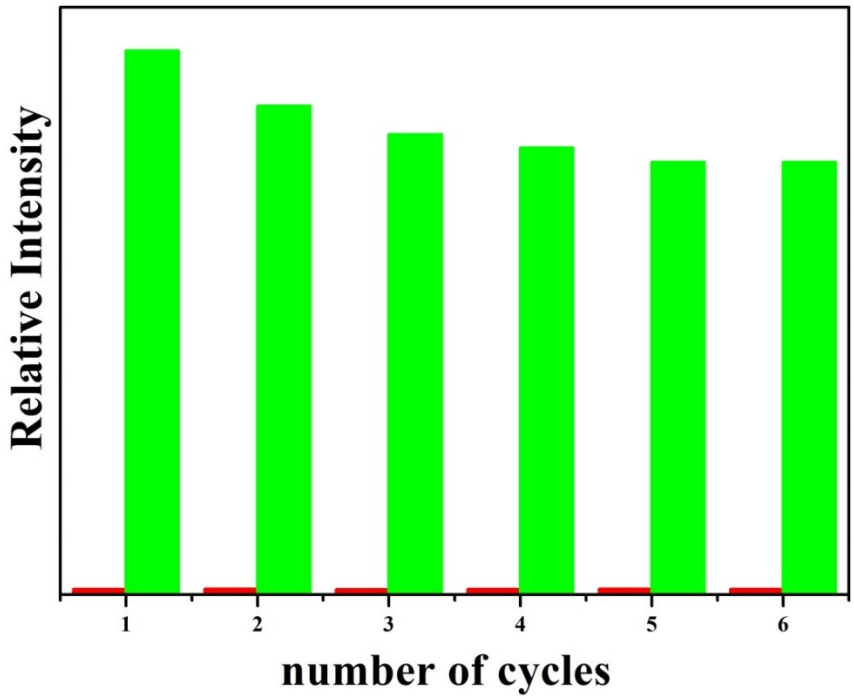

Fig. **S9** Fluorescence intensity of **La-MOF** after six recycles in Fe^{3+} solution.

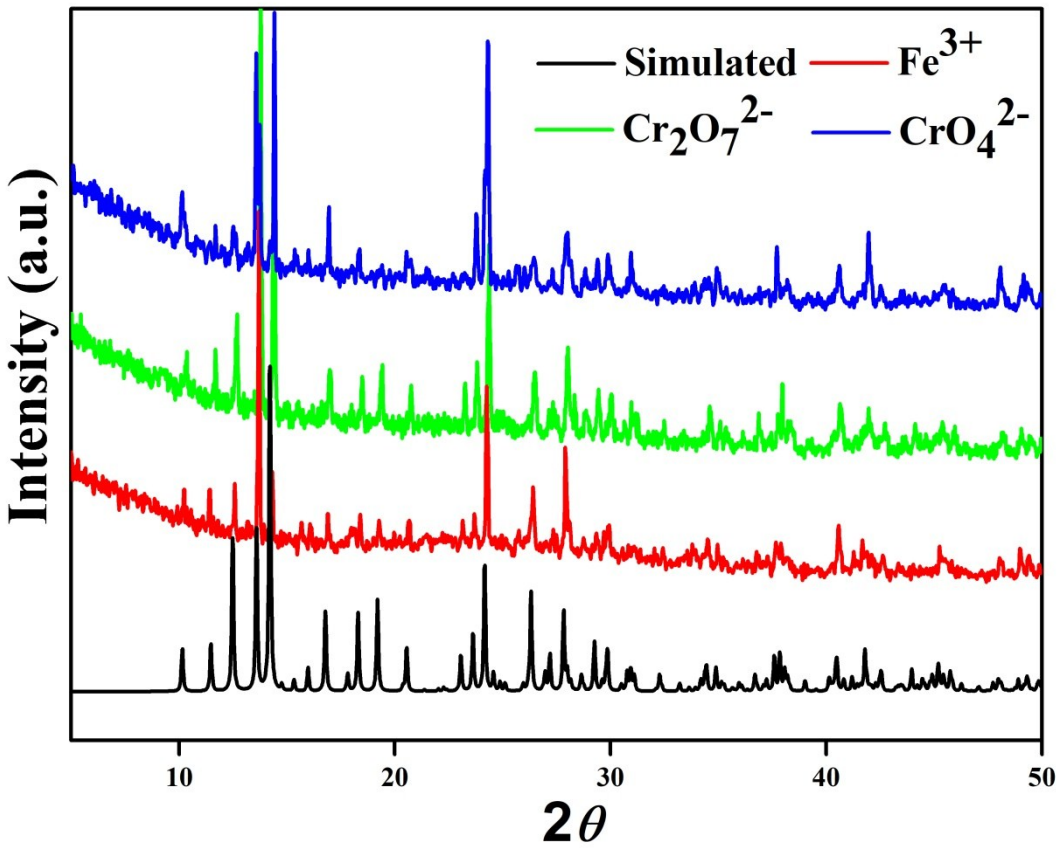

Fig. **S10** PXRD patterns of **La-MOF** treated by Fe^{3+}, $Cr_2O_7^{2-}$ and CrO_4^{2-} aqueous solutions.

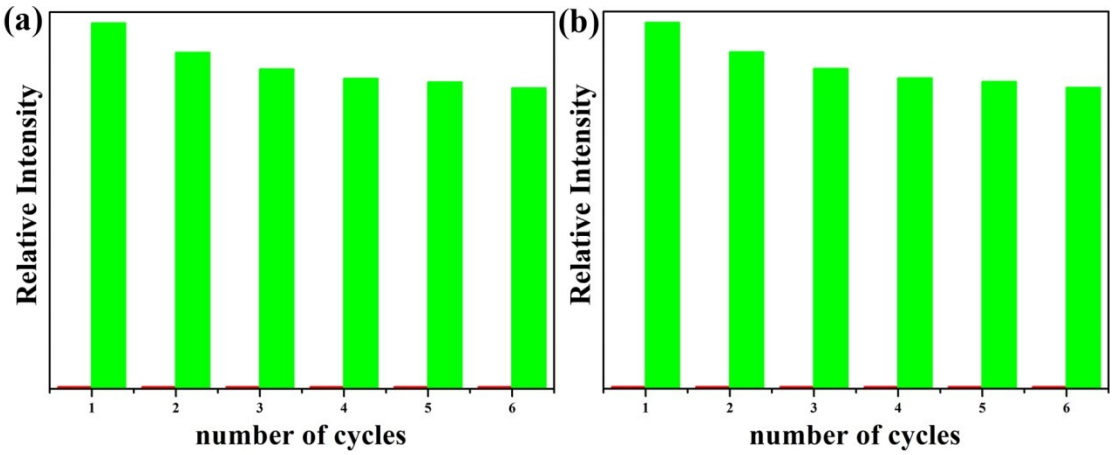

Fig. **S11** Fluorescence intensity of **La-MOF** after six recycles in (**a**) $Cr_2O_7^{2-}$ (**b**) CrO_4^{2-} solutions.

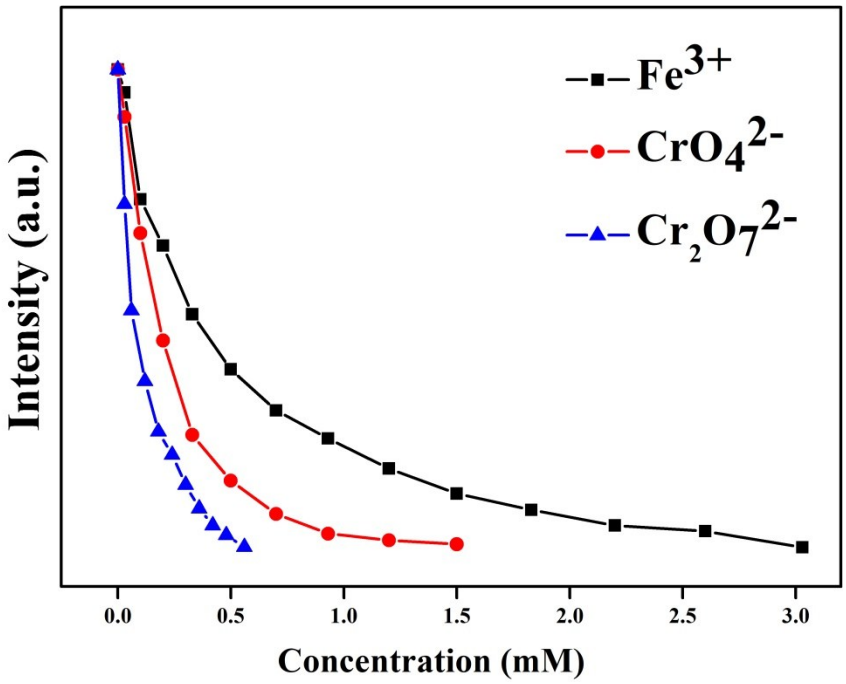

Fig. **S12** The quenching efficiency of these three ions, the fluorescence intensity changes along the ionic concentration.

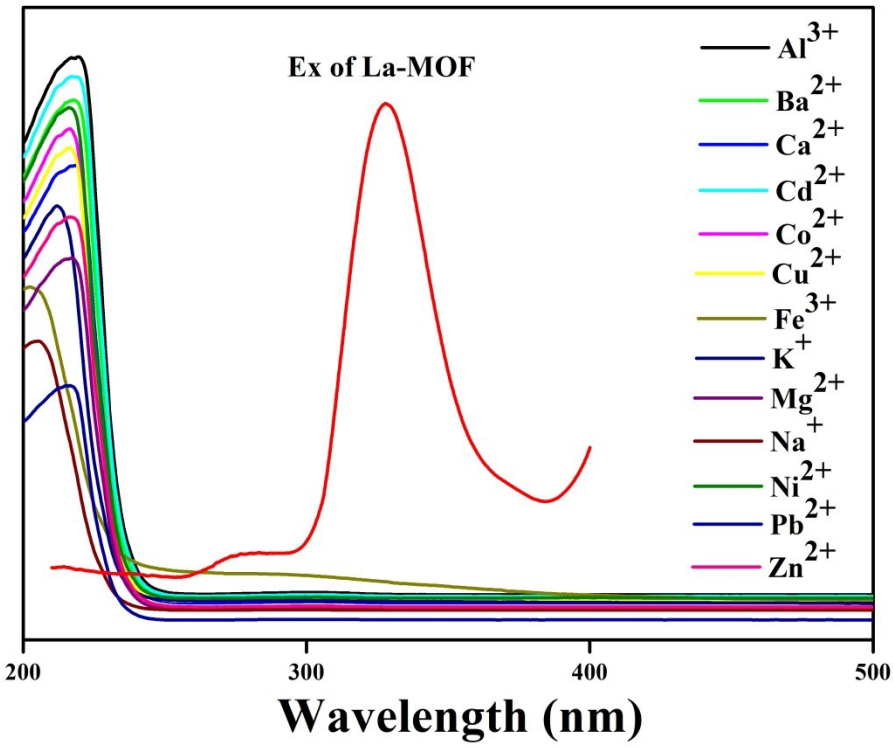

Fig. **S13** UV-Vis adsorption spectra of $M(NO_3)_n$ aqueous solutions and the excitation spectrum of **La-MOF**.

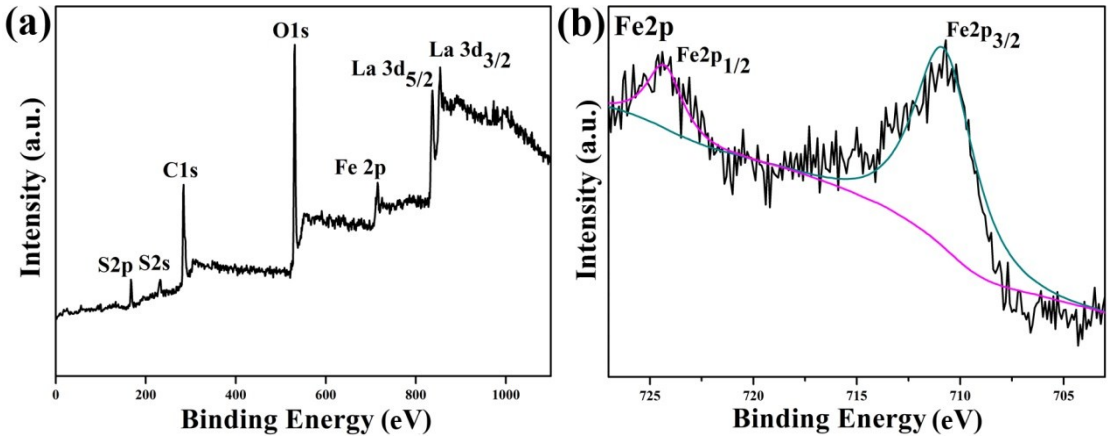

Fig. **S14** (**a**) XPS survey spectrum of **La-MOF**@Fe^{3+} and (**b**) High resolution of Fe 2p.

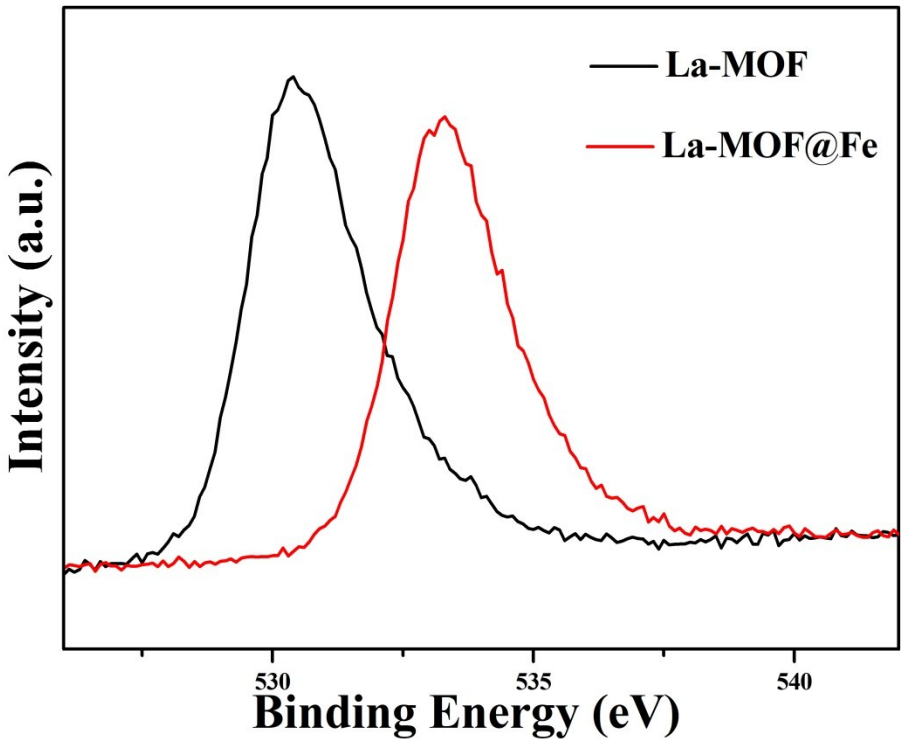

Fig. **S15** O 1s XPS spectra of the original **La-MOF** (black) and **La-MOF**@Fe^{3+} (red).

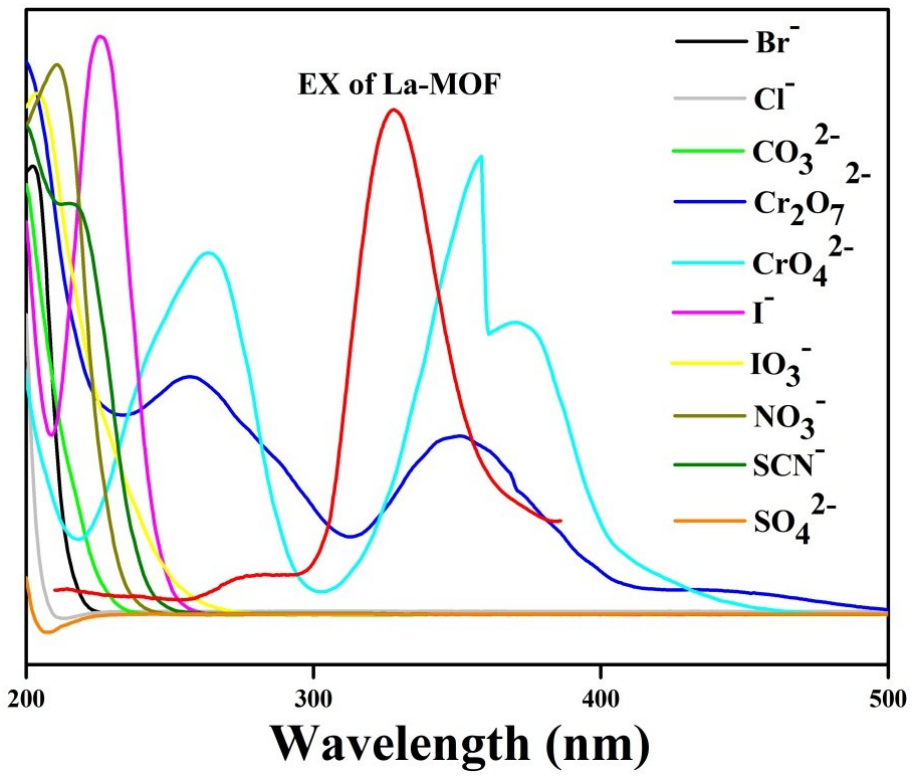

Fig. **S16** UV-Vis adsorption spectra of $K_n(A)$ aqueous solutions and the excitation spectrum of **La-MOF**.

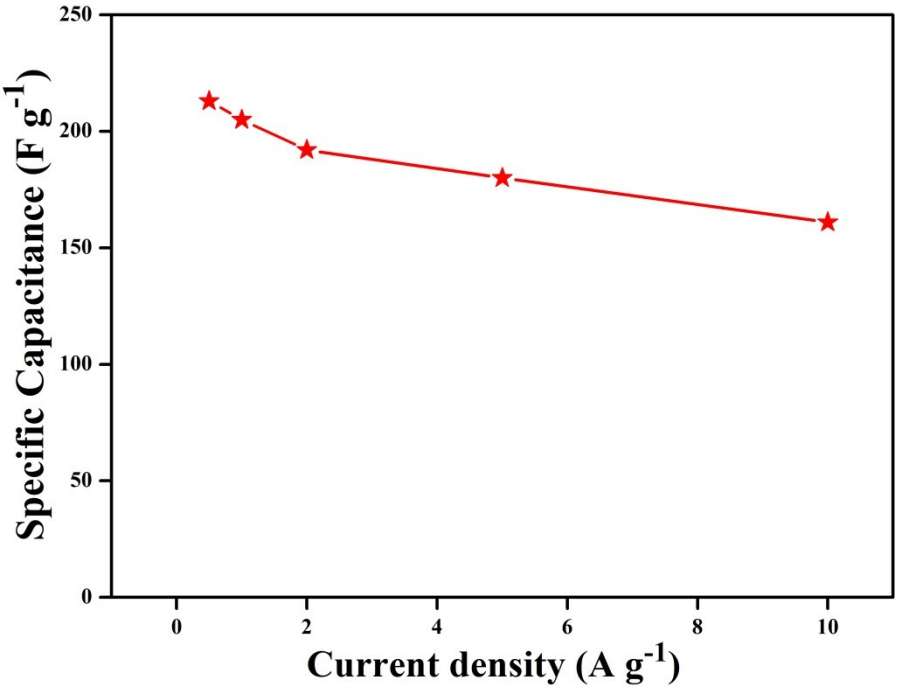

Fig. **S17** The **g**ravimetric capacitance for **La-MOF** electrode at various current densities.

Table S1 A comparison of detection capacity of **La-MOF** towards Fe^{3+} ion with other materials.

Material	Analyte	Solution	K_{sv} (M^{-1})	Reference
FJI-C8	Fe^{3+}	DMF	2.188×10^{3}	35
$[Tb_4(\mu_6\text{-}L)_2(\mu\text{-}HCOO)(\mu_3\text{-}OH)_3(\mu_3\text{-}O)(DMF)_2(H_2O)_4]_n\cdot(H_2O)_{4n}$	Fe^{3+}	DMF	1.659×10^{4}	37
$[TbL(H_2O)_2]\cdot H_2O$	Fe^{3+}	H_2O	1.9×10^{3}	38
$[Tb(HL)(H_2O)_3]\cdot H_2O$	Fe^{3+}	H_2O	2.063×10^{3}	39
$\{[Tb_4(OH)_4(DSOA)_2(H_2O)_8]\cdot(H_2O)_8\}_n$	Fe^{3+}	H_2O	3.543×10^{3}	40
$[Ln(\mu^3\text{-}cpta)(phen)(H_2O)_2]_n$	Fe^{3+}	H_2O	2.138×10^{3}	41
La-MOF	Fe^{3+}	H_2O	3.534×10^{3}	**This work**

Table S2 A comparison of detection capacity of **La-MOF** towards $Cr_2O_4^{2-}$ and CrO_4^{2-} ions with other materials.

Material	Analyte	Solution	K_{sv} (M^{-1})	Reference
$[Zn_2(TPOM)(NH_2–BDC)_2]·4H_2O$	$Cr_2O_7^{2-}$ /CrO_4^{2-}	H_2O	7.59×10^{3} /4.45×10^{3}	42
$\{[Zn(IPA)(L)]\}_n$	$Cr_2O_7^{2-}$ /CrO_4^{2-}	H_2O	1.37×10^3 /1.0×10^3	43
$\{[Cd(IPA)(L)]\}_n$	$Cr_2O_7^{2-}$ /CrO_4^{2-}	H_2O	2.91×10^3 /1.30×10^3	43
$[Eu_2(tpbpc)_4·CO_3·4H_2O]·DMF·solvent$	$Cr_2O_7^{2-}$ /CrO_4^{2-}	H_2O	1.04×10^4 /4.85×10^3	44
$\{[Cd_3(HL)_2(H_2O)_3]·3H_2O·2CH_3CN\}_n$	$Cr_2O_7^{2-}$ /CrO_4^{2-}	H_2O	6.99×10^3 /1.41×10^4	45
$[Cd(L)_2(H_2O)_2]_n$	$Cr_2O_7^{2-}$ /CrO_4^{2-}	H_2O	5.1×10^4 /1.1×10^4	46
La-MOF	$Cr_2O_7^{2-}$ /CrO_4^{2-}	H_2O	1.58×10^4 /6.722×10^3	**This work**

Table S3 Comparison of supercapacitive performance of our sample with other previously reported MOF-based electrode materials.

MOF-based materials	Specific capacitance	Current density /Scan rate	Retention (%)	Electrolyte	Reference
Cu-MOF	85 F g^{-1}	1.6 A g^{-1}	91	1 M Na_2SO_4	52
Cu-bipy-BTC	160 F g^{-1}	0.005 mA g-1	93	0.1 M $HClO_4$	53
Co-BPDC	179.2 F g^{-1}	10 mV s^{-1}	77	0.5 M LiOH	54
$[Ni(Hppza)_2]_n$	184 F g^{-1}	5 mV s^{-1}	65	2 M KOH	55
Co-MOF	206.8 F g^{-1}	0.6 A g^{-1}	98	0.5 M LiOH	56
Cu@BTC	228 F g^{-1}	1.5 A g^{-1}	89	3 M KOH	57
Ni-MOF	237 mA h g^{-1}	1 A g^{-1}	-	3 M KOH	58
La-MOF	213 F g^{-1}	0.5 A g^{-1}	92	2 M KOH	**This Work**